

Appendix A

Transformation of the Rotating to Inertial Coordinate Systems

To calculate the moment acting upon the rotor by using the angular momentum theorem, the product rule of differentiation is applied. The resulting moment in the rotating coordinate system (x',y',z') is transformed into the inertial coordinate system (x,y,z) . Therefore, the relations between the unit vectors of two coordinate systems are needed.

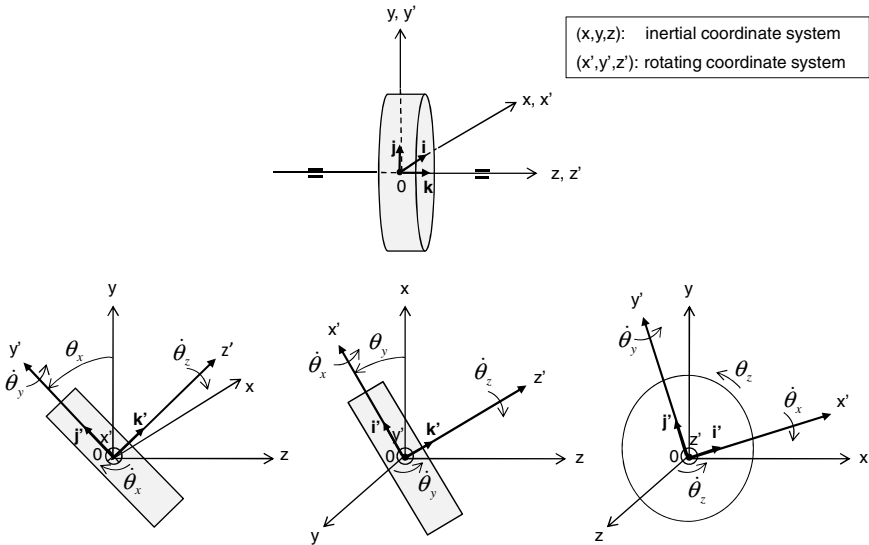


Fig. 1 Transformation between the rotating and inertial coordinate systems

Two-dimensional angular position vector θ is written in the rotating coordinate system (x',y',z') with $\theta_z = 0$.

$$\theta = \theta_x \mathbf{i}' + \theta_y \mathbf{j}' \tag{1}$$

where

θ_x , θ_y , and θ_z are the proper Euler angles in the directions x' , y' , and z' .

The relation between the unit vectors (\mathbf{i}' , \mathbf{j}' , \mathbf{k}') and (\mathbf{i} , \mathbf{j} , \mathbf{k}) of the rotating and inertial coordinate systems is derived [1].

$$\begin{pmatrix} \mathbf{i}' \\ \mathbf{j}' \\ \mathbf{k}' \end{pmatrix} = \mathbf{I} \mathbf{R}_{\theta_x} \mathbf{R}_{\theta_y} \begin{pmatrix} \mathbf{i} \\ \mathbf{j} \\ \mathbf{k} \end{pmatrix} = \mathbf{R} \begin{pmatrix} \mathbf{i} \\ \mathbf{j} \\ \mathbf{k} \end{pmatrix} \quad (2)$$

where

\mathbf{I} is the unit matrix;

\mathbf{R}_{θ_x} and \mathbf{R}_{θ_y} are the transform matrices in functions of θ_x and θ_y , respectively.

$$\mathbf{R}_{\theta_x} = \begin{pmatrix} 1 & 0 & 0 \\ 0 & \cos \theta_x & \sin \theta_x \\ 0 & -\sin \theta_x & \cos \theta_x \end{pmatrix}; \quad \mathbf{R}_{\theta_y} = \begin{pmatrix} \cos \theta_y & 0 & -\sin \theta_y \\ 0 & 1 & 0 \\ \sin \theta_y & 0 & \cos \theta_y \end{pmatrix} \quad (3)$$

The transform matrix \mathbf{R} is calculated from \mathbf{I} , \mathbf{R}_{θ_x} and \mathbf{R}_{θ_y} as follows:

$$\mathbf{R} \equiv \mathbf{I} \mathbf{R}_{\theta_x} \mathbf{R}_{\theta_y} = \begin{pmatrix} \cos \theta_y & 0 & -\sin \theta_y \\ \sin \theta_x \sin \theta_y & \cos \theta_x & \sin \theta_x \cos \theta_y \\ \cos \theta_x \sin \theta_y & -\sin \theta_x & \cos \theta_x \cos \theta_y \end{pmatrix} \quad (4)$$

Therefore,

$$\begin{cases} \mathbf{i}' = \cos \theta_y \mathbf{i} - \sin \theta_y \mathbf{k} \\ \mathbf{j}' = (\sin \theta_x \sin \theta_y) \mathbf{i} + \cos \theta_x \mathbf{j} + (\sin \theta_x \cos \theta_y) \mathbf{k} \\ \mathbf{k}' = (\cos \theta_x \sin \theta_y) \mathbf{i} - \sin \theta_x \mathbf{j} + (\cos \theta_x \cos \theta_y) \mathbf{k} \end{cases} \quad (5)$$

At small angles $\theta_x, \theta_y \ll 1$ with $\cos \theta \approx 1 - \theta^2/2$ and $\sin \theta \approx \theta$, one obtains

$$\begin{cases} \mathbf{i}' \approx \mathbf{i} - \theta_y \mathbf{k} \approx \mathbf{i} \\ \mathbf{j}' \approx \mathbf{j} + \theta_x \mathbf{k} \approx \mathbf{j} \\ \mathbf{k}' \approx \theta_y \mathbf{i} - \theta_x \mathbf{j} + \mathbf{k} \approx \mathbf{k} \end{cases} \quad (6)$$

Generally, the three-dimensional angular position vector $\boldsymbol{\theta}$ is written in the rotating coordinate system (x', y', z').

$$\boldsymbol{\theta} = \theta_x \mathbf{i}' + \theta_y \mathbf{j}' + \theta_z \mathbf{k}' \quad (7)$$

The relations of the unit vectors are formulated by the transform matrices.

$$\begin{pmatrix} \mathbf{i}' \\ \mathbf{j}' \\ \mathbf{k}' \end{pmatrix} = \mathbf{R}_{\theta_z} \mathbf{R}_{\theta_x} \mathbf{R}_{\theta_y} \begin{pmatrix} \mathbf{i} \\ \mathbf{j} \\ \mathbf{k} \end{pmatrix} \equiv \mathbf{R}^* \begin{pmatrix} \mathbf{i} \\ \mathbf{j} \\ \mathbf{k} \end{pmatrix} \quad (8)$$

with

the transform matrices \mathbf{R}_{θ_x} and \mathbf{R}_{θ_y} given in Eq. (3) and

$$\mathbf{R}_{\theta_z} = \begin{pmatrix} \cos \theta_z & \sin \theta_z & 0 \\ -\sin \theta_z & \cos \theta_z & 0 \\ 0 & 0 & 1 \end{pmatrix} \quad (9)$$

The transformation matrix \mathbf{R}^* is calculated from \mathbf{R}_{θ_z} , \mathbf{R}_{θ_x} and \mathbf{R}_{θ_y} .

$$\mathbf{R}^* = \begin{pmatrix} \cos \theta_z \cos \theta_y + \sin \theta_z \sin \theta_x \sin \theta_y & \sin \theta_z \cos \theta_x & -\cos \theta_z \sin \theta_y + \sin \theta_z \sin \theta_x \cos \theta_y \\ -\sin \theta_z \cos \theta_y + \cos \theta_z \sin \theta_x \sin \theta_y & \cos \theta_z \cos \theta_x & \sin \theta_z \sin \theta_y + \cos \theta_z \sin \theta_x \cos \theta_y \\ \cos \theta_x \sin \theta_y & -\sin \theta_x & \cos \theta_x \cos \theta_y \end{pmatrix} \quad (10)$$

At small angles $\theta_x, \theta_y, \theta_z \ll 1$ with $\cos \theta \approx 1 - \theta^2/2$ and $\sin \theta \approx \theta$, one obtains

$$\begin{cases} \mathbf{i}' \approx \mathbf{i} + \theta_z \mathbf{j} - \theta_y \mathbf{k} \approx \mathbf{i} \\ \mathbf{j}' \approx -\theta_z \mathbf{i} + \mathbf{j} + \theta_x \mathbf{k} \approx \mathbf{j} \\ \mathbf{k}' \approx \theta_y \mathbf{i} - \theta_x \mathbf{j} + \mathbf{k} \approx \mathbf{k} \end{cases} \quad (11)$$

Appendix B

Calculating Value x from X in the Log₁₀ Scale

The value x at an arbitrary ratio ξ is interpolated from the measured values X at an arbitrary ratio ξ in the log₁₀ scale, as shown Fig. 1.

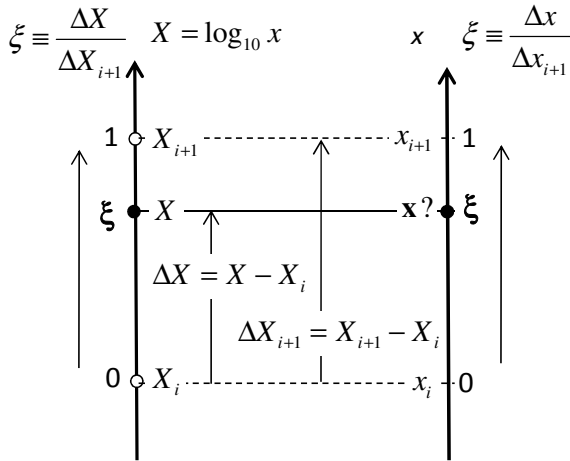


Fig. 1 Calculating value x from X in the log₁₀ scale

The intervals ΔX and ΔX_{i+1} in the log₁₀ scale are calculated.

$$\Delta X = X - X_i = \log_{10} \left(\frac{x}{x_i} \right) \quad (1)$$

$$\Delta X_{i+1} = X_{i+1} - X_i = \log_{10} \left(\frac{x_{i+1}}{x_i} \right) \quad (2)$$

Having divided Eq. (1) to Eq. (2), one obtains

$$\log_{10} \left(\frac{x}{x_i} \right) = \left(\frac{\Delta X}{\Delta X_{i+1}} \right) \log_{10} \left(\frac{x_{i+1}}{x_i} \right) = \log_{10} \left(\frac{x_{i+1}}{x_i} \right)^{\left(\frac{\Delta X}{\Delta X_{i+1}} \right)} \quad (3)$$

Thus,

$$\left(\frac{x}{x_i}\right) = \left(\frac{x_{i+1}}{x_i}\right)^{\left(\frac{\Delta X}{\Delta X_{i+1}}\right)} = \left(\frac{x_{i+1}}{x_i}\right)^\xi = 10^\xi \tag{4}$$

where

$$\xi \equiv \frac{\Delta X}{\Delta X_{i+1}} = \frac{X - X_i}{X_{i+1} - X_i}; 0 < \xi < 1 \tag{5}$$

The corresponding value x of X in the \log_{10} scale is computed from the ratio ξ according to Eq. (4) where ξ is the relative distance of X between X_{i+1} and X_i . The values x are plotted for various values ξ in case $x_i = 10^1$ in Figure 2. The results help us to calculate the value x at the ratio ξ by interpolating the measured values at the ratio ξ in the \log_{10} scale.

Table 1 Computed values x from ξ of the \log_{10} scale

ξ	x/x_i	$x = x_i \cdot 10^\xi$ for		
		$x_i = 10^0$	$x_i = 10^1$	$x_i = 10^2$
0,00	1	1,00	10,00	100,00
0,05	1,12	1,12	11,22	112,20
0,10	1,26	1,26	12,59	125,89
0,15	1,41	1,41	14,13	141,25
0,20	1,58	1,58	15,85	158,49
0,25	1,78	1,78	17,78	177,83
0,30	2,00	2,00	19,95	199,53
0,35	2,24	2,24	22,39	223,87
0,40	2,51	2,51	25,12	251,19
0,45	2,82	2,82	28,18	281,84
0,50	3,16	3,16	31,62	316,23
0,55	3,55	3,55	35,48	354,81
0,60	3,98	3,98	39,81	398,11
0,65	4,47	4,47	44,67	446,68
0,70	5,01	5,01	50,12	501,19
0,75	5,62	5,62	56,23	562,34
0,80	6,31	6,31	63,10	630,96
0,85	7,08	7,08	70,79	707,95
0,90	7,94	7,94	79,43	794,33
0,95	8,91	8,91	89,13	891,25
1,00	10	10,00	100,00	1000,00

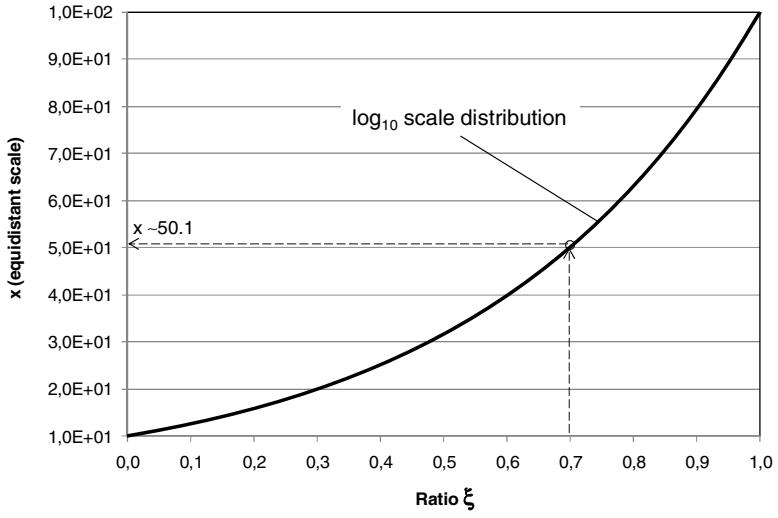


Fig. 2 Calculating x from the log₁₀ scale distribution X at $\xi = 0.7$

Appendix C

Solutions of the Characteristic Equation with Complex Coefficients

The characteristic quadratic equation with complex coefficients is derived from the vibration equation [2].

$$D(s) \equiv s^2 + (a + jb)s + (c + jd) = 0 \quad (1)$$

where

$$s = (\alpha \pm j\omega_n) \in \mathbf{C} \text{ are the complex eigenvalues;} \\ a, b, c, d \in \mathbf{R} \text{ are the real numbers.}$$

By solving the characteristic equation $D(s) = 0$, the eigenvalue s results in

$$s_{1,2} = -\left(\frac{a + jb}{2}\right) \pm \sqrt{\left(\frac{a + jb}{2}\right)^2 - (c + jd)} \quad (2) \\ = \alpha \pm j\omega_n$$

After calculating and rearranging the real and imaginary terms of the eigenvalue, one obtains

$$\alpha = -\frac{a}{2} \pm \frac{1}{\sqrt{2}} \left[\left(\frac{a^2 - b^2}{4} - c \right) + \sqrt{\left(\frac{a^2 - b^2}{4} - c \right)^2 + \left(\frac{ab}{2} - d \right)^2} \right]^{\frac{1}{2}} \quad (3)$$

and

$$\omega_n = \frac{b}{2} \pm \frac{1}{\sqrt{2}} \left[-\left(\frac{a^2 - b^2}{4} - c \right) + \sqrt{\left(\frac{a^2 - b^2}{4} - c \right)^2 + \left(\frac{ab}{2} - d \right)^2} \right]^{\frac{1}{2}} \quad (4)$$

Necessary condition for the rotordynamic stability is that the real term α of the eigenvalue must be negative (s. Section 4.2).

$$\alpha = -\frac{a}{2} \pm \frac{1}{\sqrt{2}} \left[-E + \sqrt{E^2 + F^2} \right]^{\frac{1}{2}} < 0 \quad (5)$$

within

$$E \equiv -\left(\frac{a^2 - b^2}{4} - c \right) = -\left(\frac{a^2 - b^2}{4} \right) + c \quad (6a)$$

$$F \equiv \left(\frac{ab}{2} - d \right) \quad (6b)$$

Thus, the stability condition ($\alpha < 0$) for the rotor given in eq. (5) becomes after a few calculation steps.

$$a(ac + bd) - d^2 \geq 0 \quad (7)$$

Appendix D

Normal Distribution Density Function and Probability Function

The normal distribution density function is defined with parameters \bar{z} and σ as follows:

$$p(z) = \frac{1}{\sigma\sqrt{2\pi}} \exp\left[-\frac{1}{2}\left(\frac{z - \bar{z}}{\sigma}\right)^2\right] \quad (1)$$

where

\bar{z} is the mean value of the sampling values;

σ is the standard deviation resulted from the sampling values.

$$\sigma = \sqrt{\frac{1}{(N-1)} \sum_{i=1}^N (z_i - \bar{z})^2} \quad (2)$$

within

$$\bar{z} = \frac{1}{N} \sum_{i=1}^N z_i \quad (3)$$

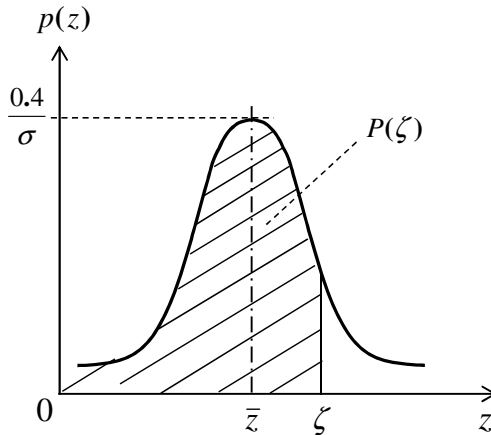


Fig. 1 Distribution density function $p(z)$ and its probability function

The normal distribution function is called the *Gaussian density function* with a bell shape; its probability distribution function is calculated by integrating $p(z)$ from $-\infty$ to ζ . This integrated value $P(\zeta)$ is the area under the bell curve, as shown in Fig. 1.

$$P(\zeta) = \frac{1}{\sigma\sqrt{2\pi}} \int_{-\infty}^{\zeta} \exp\left[-\frac{1}{2}\left(\frac{z-\bar{z}}{\sigma}\right)^2\right] dz \quad (4)$$

By substituting z by the new dimensionless variable,

$$c \equiv \frac{z-\bar{z}}{\sigma} \quad (5)$$

the normal distribution function $p(z)$ is written in

$$p(c) = \frac{1}{\sqrt{2\pi}} \exp\left[-\frac{c^2}{2}\right] \quad (6)$$

The new probability function is written in the new variable c .

$$P(c) = \frac{1}{\sqrt{2\pi}} \int_{-\infty}^c \exp\left[-\frac{1}{2}c^2\right] dc \quad (7)$$

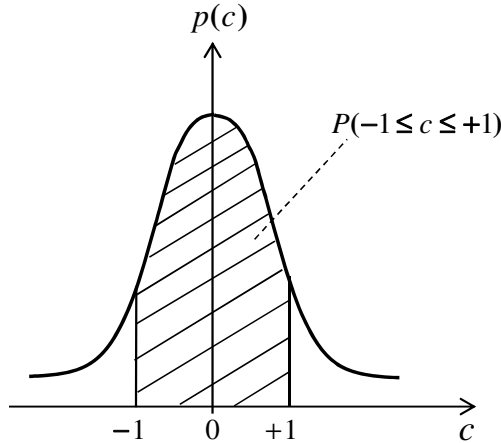


Fig. 2 Distribution density function $p(c)$ and its probability function $P(c)$

Thus,

$$P(-1 \leq c \leq +1) = \frac{1}{\sqrt{2\pi}} \int_{-1}^{+1} \exp\left[-\frac{1}{2}c^2\right] dc \quad (8)$$

The probability distribution values for various parameters are calculated from Eq. (8).

$$\left\{ \begin{array}{l} P(-1 \leq c \leq +1) = 68.3\% \\ P(-2 \leq c \leq +2) = 95.4\% \\ P(-3 \leq c \leq +3) = 99.7\% \\ P(-4 \leq c \leq +4) = 99.99\% \end{array} \right. \quad (9)$$

This result indicates that a production with $\pm 3\sigma$ would deliver 99.7% of the products that fulfill the given lowest and highest tolerances.

References

1. Adams Jr., M.L.: Rotating Machinery Vibration. CRC, Taylor and Francis (2001)
2. Muszýnska, A.: Rotordynamics. CRC, Taylor and Francis (2005)
3. Taylor, J.R.: An Introduction to Error Analysis. University Science Books (2005)

Further Readings

1. Adams Jr., M.L.: Rotating Machinery Vibration. CRC, Taylor and Francis (2001)
2. Bently, D.E., Hatch, C.: Fundamentals of Rotating Machinery Diagnostics. Bently Pressurized Bearing Press (2002)
3. Childs, D.: Turbomachinery Rotordynamics. J. Wiley and Sons Inc. (1993)
4. Den Hartog, J.P.: Mechanical Vibrations. McGraw-Hill (1956)
5. Ehrich, F.: Handbook of Rotordynamics. Krieger Publishing Company (2004)
6. Gasch, R., Nordmann, R., Pfuetzner, H.: Rotordynamik, vol. 2. Auflage, Springer (2006)
7. Genta, G.: Dynamics of Rotating Systems. Springer, Heidelberg (2005)
8. Goodwin, M.J.: Dynamics of Rotor Bearing Systems. Thomson Learning (1989)
9. Gunter, E.J.: Dynamic Stability of Rotor-Bearing Systems. NASA SP-113 (1966)
10. Hori, Y.: Hydrodynamic lubrication. Springer, Heidelberg (2006)
11. Kraemer, E.: Rotordynamics of Rotors and Foundations. Springer, Heidelberg (1993)
12. Lee, C.W.: Vibration Analysis of Rotors. Kluwer Academic (1993)
13. Muszýnska, A.: Rotordynamics. CRC, Taylor and Francis (2005)
14. Neville, F., Rieger, N.F.: Balancing of Rigid and Flexible Rotors. Shock and Vibration Information Center (1986)
15. Rao, J.S.: Rotor Dynamics, 3rd edn. New Age Intl. Publishers (2007)
16. Rieger, N.F.: Rotordynamics 2 - Problems in Turbomachinery. CISM Courses and Lectures No. 297 (1988)
17. Rieger, N.F.: Balancing of Rigid and Flexible Rotors. U.S. DoD (1986)
18. Rieger, N.F., Crofoot, J.F.: Vibrations of Rotating Machinery. Vibration Institute (1977)
19. Schweitzer, G., et al.: Magnetic Bearings. Springer, Heidelberg (2009)
20. Vance, J.: Rotordynamics of Turbomachinery. J. Wiley and Sons Inc. (1988)
21. Vance, J., Zeidan, Murphy, B.: Machinery Vibration and Rotordynamics. J. Wiley (2010)
22. Tondl, A.: Some problems of Rotor Dynamics. Chapman & Hall (1965)
23. Yamamoto, T., Ishida, Y.: Linear and Nonlinear Rotordynamics. J. Wiley and Sons Inc. (2001)
24. Wen, J.C., Gunter, J.: Introduction to Dynamics of Rotor-Bearing Systems. Eigen Technologies ETI (2001)
25. Wowk, V.: Machinery Vibration and Balancing. McGraw-Hill (1995)

Index

- Abbott curve 285–288, 290
- abrasive friction 293, 294
- adhesive friction 279, 294, 299
- airborne noises 221, 280
- air-fuel ratio 12
- aliasing 225, 227
- angular momentum 102–107, 171, 307
- angular velocity 102, 104, 107, 108, 171, 179–181
- anisotropic bearings 44, 45, 113, 121
- anti-aliasing 228
- asperities 134, 279, 280, 289, 290, 299, 300, 302
- axial thrust 127, 135–137, 139, 140, 142

- backward whirl 39, 61, 117
- ball passing frequency 187
- banana shape 56
- beat phenomena 217
- bifurcation point 72, 73, 76, 77, 82
- bimodal method 194, 231
- biturbocharger 4
- boundary lubrication 134, 144, 275, 279, 299, 302
- brake specific fuel consumption 16

- Cameron and Vogel equation 148, 232, 270, 271
- Campbell diagram 39, 40, 41, 104, 115–117, 121, 197, 240
- carrier frequency 215, 218, 219
- cavitating squeeze oil film 182–185
- characteristic equation 65, 68–70, 79, 118, 194, 195, 209, 211, 315
- choke flow 23
- circulant damping 106, 109, 111
- circulant stiffness 109, 111

- complex dynamic stiffness 93, 94, 96, 262, 263
- complex eigenvalue 60, 61, 64, 79, 208, 209, 313
- compressor efficiency 18, 19
- compressor-stall-related noise 221
- constant tone 221, 223
- convolution 47, 48, 87, 200
- core roughness depth 287, 288, 290
- core unit 128
- corrected mass flow rate 23, 26
- couple unbalance 35, 106, 248, 249, 252
- critical frequency 59, 91, 117, 199, 203, 211, 240
- critically damped 66, 97
- cutoff wavelength 283

- damping coefficient 66, 68, 101, 169, 182–185, 193, 208, 230
- damping ratio 65–67, 97, 100, 101
- decay rate 60, 61, 65–67
- delivery acceleration response 265
- destabilizing force 59, 201, 208, 223
- discrete fourier transform 227, 237
- downsized engine 2
- dynamic unbalance 249, 252
- dynamic viscosity 131, 133, 136, 145, 148, 149, 158, 164, 170, 171, 173, 183–186, 232, 269–274, 276, 277

- eccentricity 34, 35, 54, 59, 71, 108, 157, 158–161, 163, 164, 169, 182–186, 199, 204, 205, 207, 208, 223, 224, 234, 238, 242, 248, 249, 252, 258, 260, 261, 262, 275, 277
- eddy-current sensor 41
- EDTC, 8, 9

- effective temperature 148, 152, 174
 eigenfrequency 39, 60, 91, 95, 116,
 119, 121, 197, 261, 267
 eigenmode 36, 39, 123, 124
 eigenvector 68, 95, 194, 195
 end oil damper 182–184
 equilibrium points 73, 79, 80
 erosive wear 300, 304
 evaluation length 280, 281, 283, 284
 exhaust gas recirculation 2
- fast fourier transform 225
 fatigue wear 303
 flexible rotor 36, 39, 99–101, 124, 125,
 230, 236, 257, 258, 263, 268
 floating ring bearing 156, 169, 170, 172
 fluid circumferential 198, 204
 fluid-film bearings 59
 focus 74, 75, 77
 forced vibration responses 39, 95
 forward whirl 39, 45, 47, 48, 51, 54, 56,
 61, 104, 116, 119, 121, 123, 124, 199,
 200, 206, 207, 234, 240
 Fourier transform 225
 fractional frequency orders 51, 57, 200
 free vibration response 39, 60, 68, 95
 frequency spectrum 40, 45, 50, 52, 54,
 201, 231
 fretting wear 300
 friction loss 21
 fuel combustion efficiency 12
 fuel mileage 13, 274
 fundamental train frequency 186
- gyroscopic effect 63, 64, 67, 101, 102,
 104, 109, 116, 118, 230
 gyroscopic moment 104, 109
- half-frequency whirl 46, 207
 harmonic vibrations 37, 38
 heating value 12
 heavy rub 51, 200, 211
 Hersey number 133, 134
 high-pressure EGR 2, 3, 6
 homogeneous solutions 60
 Hopf bifurcation 41, 61, 72, 73, 76, 77,
 79, 82, 84, 235
 HTHS viscosity 272, 274, 275
 hydrodynamic lubrication 132, 133,
 144, 157, 279, 280, 299
- impulse momentum 104, 208
 incommensurate frequencies 38, 82
 Influence Coefficient Method 258, 261,
 262, 267
 influential parameters 152, 154, 174
 initial unbalance 250–252
 inner loops 48, 51, 234
 in-phase couple 35, 256
 instability 40, 59, 61, 92, 117, 155, 191,
 192, 199, 204, 208, 210, 211, 223,
 224, 240, 275
 inverse discrete fourier transform 227
 irrational frequency orders 46, 49, 51
 isentropic enthalpy 20, 21
 isentropic process 18–20
- Jacobian matrix 79
 Jeffcott rotor 62, 63, 67, 94, 96,
 109–111, 113
- kinematic viscosity 269, 270
- Lagrange function 111
 Lagrangian coordinates 111
 lateral 35, 109–111, 118, 124
 lateral kinetic energy 92
 limit acceleration responses, 267
 limit cycle 40, 41, 61, 73–77, 93, 234,
 236–238, 266
 linear rotordynamics 39, 41, 61, 114,
 115, 121, 161, 240
 Lissajous curves 40, 43
 long bearings 159, 184
 low-cycle fatigue 4, 191, 301
 low-end torque 5, 27, 93, 127, 142, 154,
 173
 low-pressure EGR 3, 4
 low-speed balancing 35, 246, 251,
 254–256
 LSB 215, 216, 219, 220
 lubrication regions 132, 277, 279, 280
- Mach number 23
 material ratio 285
 maximum roughness depth 284, 285
 mean effective pressure 15, 16
 mean roughness 283–285
 mean roughness depth 143, 144, 287
 mechanical efficiency 21, 22, 28
 mechanical wear 302

- misalignment 40, 54, 56, 57, 106, 108, 110, 121, 192, 197, 200, 201, 211, 217, 252, 255, 266
- mixed lubrication 134, 137, 143, 144, 150, 152, 279
- modal balancing 258, 267
- modal matrix 196
- modulations 40, 121, 129, 186, 197, 201, 213, 215, 217, 220
- Mohr's circle 298
- moment unbalance 108, 252, 253
- Navier-Stokes equations 130
- Neimark-Sacker bifurcation 82–84
- Newton's second law 137
- node 74
- noises 101, 117, 129, 154, 169, 174, 176, 221, 222, 280
- non-autonomous systems 82, 87
- non-cavitating oil film 159, 160
- non-conservative generalized forces 111
- nonlinear rotordynamics 40, 41, 43, 71, 74, 92, 121, 197, 201, 228, 238, 240, 266
- Nyquist criterion 228
- Nyquist frequency 225, 228, 229
- oil whip 59, 92, 117, 197, 203, 204, 210, 211, 240
- oil whirl 40, 46, 47, 49–51, 59, 129, 154, 169, 176, 197–199, 201, 203, 204, 207, 208, 210, 211, 215, 217, 221, 233, 237–239, 244, 280
- onset of instability 59, 61, 92
- orthotropic bearings 44, 63
- out-of-phase couple 35, 256, 257
- overall efficiency 21
- overdamped 66
- oxidative wear 304
- particular solution 39, 95
- performance map 23, 26
- periodic vibrations 39, 40, 46, 47, 49, 51, 52, 54, 72–74, 76, 78, 82, 84, 87
- pitch diameter 180, 186, 187
- Poincaré map 38, 82, 87, 88
- polar mass inertia moment 28, 102, 103, 117
- pressure ratio 3, 4, 6, 7, 21, 22, 23, 27
- pulsation noise 221
- quasi-periodic vibrations 38, 82, 84
- radial bearings 2, 84, 93, 127, 131, 154–156, 161, 191, 204, 221, 223, 230, 231, 280
- Rayleigh dissipation function 111
- reduced peak height 287–289
- reduced valley height 287, 288
- repelling torus 82
- residual unbalance 35, 101, 113, 154, 222, 249, 255, 256
- resonance 34, 40, 59, 91, 92, 98, 100, 114–116, 121, 123, 124, 128, 169, 174, 176, 197, 201, 203, 238, 248, 266, 280
- response time 27, 28
- revolution 47, 48, 200
- Reynolds lubrication equation 130, 131, 135, 146, 155, 156, 158, 161, 171
- Reynolds numbers 130
- rigid rotors 247
- ring speed ratio 171–174, 198, 199, 203, 237, 239, 273
- rolling wear 300
- rolling-element bearings 28, 127, 129, 175, 182, 186
- root mean square roughness 284
- rotating floating ring bearings 28, 121, 127, 130, 156, 173, 174, 192, 222, 229, 230, 232, 240, 273
- rotating-blades-related noise 221
- rotational kinetic energy 46, 116
- Routh-Hurwitz criterion 60, 67, 69, 70
- Runge-Kutta scheme 196, 231
- run-up 111, 114, 237
- sampling length 281, 283, 284
- self-excitation instability 59, 92, 204
- shear rate 270, 272–274, 292
- shear stress 134, 272–274, 292, 294, 295, 297, 298, 300
- shop balancing 35, 108, 222, 247, 249
- short bearings 159, 161, 164, 182
- side-band frequencies 201, 211
- single-stage turbocharger 2–4, 6–8
- singular points 73, 79
- sliding wear 298
- slurry wear 298, 299
- Sommerfeld number 164, 165, 169, 231
- sonic speed 23
- squeeze-film term 131, 132

- stability 39, 41, 60, 61, 64, 68–74, 76, 77, 80–82, 84, 86, 91, 154, 174, 191, 192, 209–211, 280, 315
- static unbalance 248, 249, 252
- stiffness coefficient 35, 44, 46, 59, 63, 64, 71, 94, 99, 100, 109, 118, 193, 199, 201, 208, 209, 211, 223, 230
- stoichiometric combustion 13
- Stribeck curve 132, 134, 135, 277–279, 299
- subcritical bifurcations 76, 77, 79
- subcritically damped 66
- subsynchronous 40, 46–49, 51, 52, 54, 87, 92, 121, 129, 187, 197, 200, 204, 223, 234, 237, 238, 243, 244
- supercritical bifurcations 76, 77, 79
- supersynchronous 35, 38, 40, 44, 48, 54, 87, 121, 187, 200, 211
- surface roughness 137, 144, 150, 191, 277, 278, 280–291, 295
- surge 140
- threshold of instability 61, 211
- thrust bearing 2, 127, 135–137, 139, 143–147, 149, 150, 152, 191, 192, 232, 280, 300–302
- torus bifurcation 82
- total enthalpy 17
- total pressure 17
- total temperature 17
- transcritical bifurcations 76, 77
- transfer impedance 93, 212, 262, 263
- transverse mass inertia moment 108, 123
- trim balancing 35, 101, 191, 222, 240, 248, 258, 262, 266, 267
- turbine efficiency 19, 20, 27, 28
- turbocharger equation 21–23
- two-stage turbochargers 2, 5, 7
- two-times ball spin frequency 187
- U2W ratio 33, 34
- unbalance 248
- unbalance change 221, 222, 266, 267
- unbalance moment 106–109, 249, 252, 253
- unbalance whistle 117, 154, 221, 248, 257, 266, 267, 280
- underdamped 66, 100
- USB 215, 216, 219, 220
- vibration mode 175, 203, 223, 236, 258–261
- viscosity index 276
- VTG 9–12, 19, 140, 141
- waste gate 6, 9, 10, 19, 128
- Waterfall diagram 40–42, 199–203, 212, 217, 218, 222, 225, 231, 237, 238, 255
- wedge-velocity term 131
- Woehler curve 303